Original Article

The tumor shape changes of nasopharyngeal cancer during chemoradiotherapy: the estimated margin to cover the geometrical variation

Wenyong Tan[1,2]*, Jianzeng Ye[1]*, Ruilian Xu[1], Xianming Li[1], Wan He[1], Xiaohong Wang[2], Yanping Li[2], Desheng Hu[2]

[1]Department of Oncology, the Second Clinical Medical College (Shenzhen People's Hospital), Ji'nan University, Dongmen, Shenzhen 518020, China; [2]Department of Radiation Oncology, Hubei Cancer Hospital, Zhuodaoquan, Wuhan 430079, China

*These authors contributed equally to this work.

Correspondence to: Wenyong Tan. Department of Oncology, the Second Clinical Medical College (Shenzhen People's Hospital), Ji'nan University, No. 1017, North Road, Dongmen, Shenzhen 518020, China. Email: tanwyym@hotmail.com; Ruilian Xu. Department of Oncology, the Second Clinical Medical College (Shenzhen People's Hospital), Ji'nan University, No. 1017, North Road, Dongmen, Shenzhen 518020, China. Email: xuruilian@126.com.

Background: Considerable geometrical change occurs during chemoradiotherapy (CRT) course of nasopharyngeal carcinoma (NPC). This aim of this study was to quantify the volumetric and surface variability of the target volumes (TV) and to estimate the expanded margin to maintain acceptable geometrical coverage.

Methods: Twenty patients with locally advanced nasopharyngeal cancer underwent one planning CT (pCT) and six weekly repeated CT (rCT) scans during the treatment course of definitive CRT. The TV included the gross tumor volume (GTV) of the primary tumor, large (shortest diameter >3.0 cm) and small (diameter >1 cm and ≤3 cm) positive neck lymph nodes, and low-risk clinical target volume ($CTV_{\_Lr}$) that were delineated manually on the pCT and each rCT. When comparing TV in pCT ($V_{\_pCT}$) and TV in rCT ($V_{\_rCT}$), the overlapping index (OI), Dice similarity coefficient (DSC), shortest perpendicular distance (SPD), and overall standard deviation (overall SD) were calculated to present the geometric changes. An isotropical margin was expanded outward around $CTV_{\_Lr}$ in pCT to establish the mimic planning target volume (PTV). An OI ≥0.95 was defined as acceptable geometrical coverage.

Results: For all TV, DSCs decreased, and the SPDs and overall SD increased with the increasing number of fractions delivered. The DSCs of all gross TV were <70% after the third week. The mean SPDs were 1.5–2.5 mm in the first week and 5.2–6.2 mm in the last week. The OI and DSC in concurrent CRT were smaller than those in the sequential therapy; and similarly the SPD and overall SD in the concurrent therapy were larger than those in the sequential one. To maintain >95% geometrical coverage, a 2-mm additional margin could maintain the coverage throughout the treatment course and a 1-mm margin could maintain the desired coverage if there is an adaptive re-planning no later than the third week of the treatment course.

Conclusions: Both volumetric coverage and surface of the tumour underwent the progressive changes during the treatment course of CRT. One to two mm as the expanded margin to establish the PTV is required to maintain >95% geometrical coverage.

Keywords: Nasopharyngeal carcinoma (NPC); chemotherapy; radiotherapy; geometrical changes; margin

Submitted Jan 30, 2016. Accepted for publication Mar 10, 2016.
doi: 10.21037/qims.2016.03.07
View this article at: http://dx.doi.org/10.21037/qims.2016.03.07

Introduction

The introduction of image-guided intensity-modulated radiotherapy (IMRT) for nasopharyngeal carcinoma (NPC) further improves the precision of radiation delivery (1,2). For head and neck cancer including NPCs, however, considerable geometric changes can occur due to tumor shrinkage and weight loss, water and fat re-distribution, etc., throughout the course of IMRT (3-5). Therefore, additional efforts are needed to optimize the radiation dose delivered to the target volumes (TV) and organs at risk (5-12). In addition, a gradual volumetric loss and the shift of the center of mass of the gross tumor volume (GTV) and clinical target volume (CTV) at several time-points have been quantified with repeated imaging in previous studies (4,5,12). Some studies have demonstrated the necessity of adaptive re-planning at regular fixed intervals (11,13-16). However, the optimal timing (17), algorithms of re-planning (18), and final clinical benefit (16,19) remain unclear. Previous studies have suggested the optimal timing of re-planning was before the 15th (11,16), 20th (6), or 25th (10,14) treatment fraction, with rather arbitrariness. Effective timing of re-planning should depend on the geometrical coverage variations and should be individualized during IMRT (4).

Consecutive geometric variability including shape variation would probably improve the accuracy of adaptive radiotherapy (4,5). Recently, deformable imaging registration (20-22), implanted markers (23), and various 3-dimensional statistical shape models (24) have been used to evaluate the shape variability of a contour. The overlapping index (OI), Dice similarity coefficient (DSC) (20,21), and surface deformations (23) between images could be used as potential metrics to evaluate shape variability. This information on shape variation during the treatment course helps to determine re-planning timing and re-delineation of TVs (23). We previously reported the consecutive volumetric and positional changes of TVs during chemotherapy and IMRT for 20 patients with locally advanced NPC (4). Using serial repeat CT scans as described in the previous pilot study to mimic TV variations in the context of image-guided IMRT (4), this report presents the geometrical coverage and the surface changes of TVs and estimates the necessary margin expanded from the CTV to maintain acceptable geometrical coverage throughout the chemoradiotherapy (CRT) treatment course.

Materials and methods

Imaging acquisition and registration

The acquisition of images was reported in a previous study (4), which was approved by the ethical committee of Hubei Cancer Hospital and all patients had a written informed consent before the image acquisition. Briefly, 20 consecutive patients (15 men, 5 women) with locally advanced NPC received a contrast enhanced planning CT (pCT) scan at baseline and six weekly repeated CT (rCT) scans (at the 5th, 10th, 15th, 20th, 25th, and 30th RT fraction) without contrast during the course of chemotherapy and IMRT (4). Briefly, 13 patients received concurrent CRT, and 7 received sequential chemotherapy and radiotherapy. Among concurrent subgroup, seven received cisplatin and 5-fluorouracil for 3 cycles, five received with weekly cisplatin and another with weekly cetuximab. In sequential CRT, 2 cycles of induction chemotherapy and another 2 cycles of adjuvant chemotherapy with cisplatin and 5-fluorouracil were given to 5 patients, and the other 2 patients were treated with docetaxel and cisplatin (4). At each rCT scanning, the radiation doses delivered to the tumor were approximately 10, 20, 30, 40, 50, and 60 Gy, respectively. Before the manual delineation of TVs in the axial pCT and rCT images, each rCT was rigidly registered to its respective pCT via a research software (WALDMATC) developed in the department of Radiation Oncology, The Netherlands Cancer Institute, Amsterdam, Netherlands (4). This software could be used to the multimodal imaging registration and radiation dose calculation, etc. for the adaptive radiation therapy. The registration was based on bone match inside a rectangular-shaped region of interest which was large enough to cover the whole low-risk CTV ($CTV_{\_Lr}$) and its additional margin, i.e., planning target volume (PTV). This rigid registration was done in a similar fashion to daily image-guided RT alignment in our protocol (4). The accuracy of the registration was evaluated by visual inspection the radiation oncologist (W Tan).

Definition of the tumor and the treatment delivered

TVs were used as surrogate measures to estimate tumor shape variations. The TVs included the GTV of the primary tumor, large positive lymph nodes (shortest diameter >3 cm), small lymph nodes (diameters >1 cm and ≤3 cm), and elective $CTV_{\_Lr}$. These TVs were defined as $GTV_{\_T}$, $GTV_{\_Nl}$, $GTV_{\_Ns}$, and $CTV_{\_Lr}$, respectively. The detailed definitions

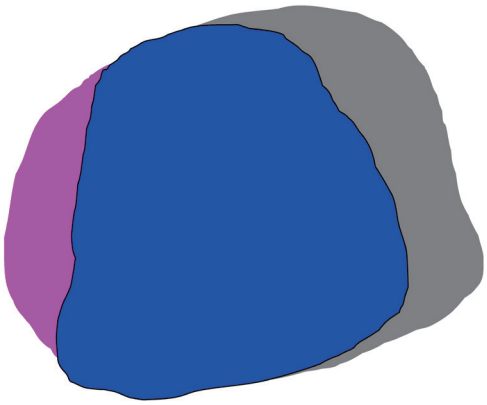

Figure 1 Schematic diagram of a target volume on pCT and rCT scans. TV was manually delineated on pCT [$TV_{\_pCT}$ (gray + blue)] and rCT [$V_{\_rCT}$ (pink + blue)] scans; common [$V_{\_common}$ (blue)] and union [$V_{\_union}$ (gray + blue + pink)] volumes are shown from a single rCT axial slice. The OI of $V_{\_rCT}$ on rCT scan was calculated by $V_{\_common}/V_{\_pCT}$, which presented the ratio of common volume and the volume of the targets in pCT. Dice similarity coefficients were calculated as $2\times V_{\_common}/(V_{\_rCT} + V_{\_pCT})$. pCT, planning CT; rCT, repeat CT; TV, target volume; OI, overlapping index; V_{rCT}, the volume in the rCT; $V_{\_common}$, common volume; $V_{\_pCT}$, volume in pCT.

of these TVs were described previously (4). $CTV_{\_Lr}$ should cover the GTV of the primary tumor and positive nodes, as well as the regions with possible microscopic disease and nodal level, as recommended by consensus (4). The individualized prescribed dose to the GTV of the primary tumor and positive lymph nodes was 69.3–72.6 Gy, that to the high-risk CTV was 59.4–62.7 Gy, and that to the PTV (3 mm expanded from $CTV_{\_Lr}$) was 54 Gy; the IMRT planning design was described in a previous study (4). All IMRTs were delivered in 33 daily fractions and 5 fractions per week. This study was designed only to document and calculate the TV shape changes during the treatment course; the actual RT delivered to patients in the following weeks remained unchanged.

Volumetric and surface variations related parameters of TVs

In radiation treatment, the differences between two contours were usually measured by volume overlap and contour surface distance (25). In this study, both the volume overlapping parameters and the TV surface distance were used as metrics to quantify the shape differences between TVs. When comparing a TV that was delineated manually by pCT and that of its respective rCT, the volume in the rCT ($V_{\_rCT}$), the volume in the pCT ($V_{\_pCT}$), and their common volume ($V_{\_common}$) were calculated by a research software (4,26). The volume overlapping parameters included OI and DSCs, which were calculated as $V_{\_common}/V_{\_rCT}$ and $2\times V_{\_common}/(V_{\_rCT} + V_{\_pCT})$ respectively (27). OI measured the fraction of $V_{\_common}$ that overlapped with the delineated TV on rCT (*Figure 1*). Larger OI values indicated better matches to the delineated TVs on pCT images (27). DSC was evaluated to quantify the overlapping ratio between two TVs. The value of OI and DSC ranged from 0 to 1. A value of 1 indicated a perfect overlap, and 0 indicated no overlap. In all of these overlapping analyses, we did not take the delineation uncertainty and imaging misalignment into account.

The surface distance [shortest perpendicular distance (SPD)] was used to represent the shape presentation (24). To calculate the 3-dimensional SPD, each point on the surface of the TV was first established from the pCT. The closest surface point of the corresponding TV in rCT was calculated in a direction perpendicular to the corresponding surface point established in pCT. The distance between these two points was the SPD (26,28). Each point in rCT had a SPD, and the mean SPD and standard deviation (SD) were computed (24). The variation in distance to all points describing the mean surface was expressed as an overall SD, which was a measure of overall TV surface variation in CT images acquired at different time-points (28,29).

Establishing PTV to estimate the expanded margin

During the course of IMRT, a safety margin is required to ensure that the planned dose is actually delivered to the TV for almost all patients (29). Around the $CTV_{\_Lr}$ in pCT, margins were isotropically expanded outward by 1, 2, 3, 4, and 5 mm to establish PTV_{-x} (x =0, 1, 2, 3, 4, 5), respectively and PTV_{-0} was the $CTV_{\_Lr}$ delineated in pCT. The total increase of PTV volume and increase per millimeter were respectively calculated by $(V_{\_PTV\_x} - V_{\_PTV\_0})/V_{\_PTV\_0} \times 100\%$ and $(V_{\_PTV\_x} - V_{\_PTV\_x\text{-}1})/V_{\_PTV\_x\text{-}1}$ (x =1, 2, 3, 4, 5). To estimate the expanded margin, PTV_{-x} (x =0, 1, 2, 3, 4, 5) was compared with its $CTV_{\_Lr}$ in rCT. The OI of the volume of PTV_{-x} (x =1, 2, 3, 4, 5) and $CTV_{\_Lr}$ in rCT, as well as its 95% confidence interval (95% CI), were calculated. For the OI, the lower limits of the 95% CI higher than 0.95 were arbitrarily defined as the acceptable geometrical coverage (29). The expanded margin established PTV that could have more than 95% geometrical coverage was defined as the expected

margin, without taking the delineation and registration uncertainties and set-up performance into account.

Statistical analysis

One-way analyses of variance were used to compare OI, DSC, and mean SPD among weeks. Differences between concurrent and sequential CRT were compared using the Student's *t*-test. All tests were two-tailed, and a 5% significance level was used when establishing statistical significance. The Statistical Package for Social Sciences (SPSS version 20.0; IBM Corporation, Armonk, NY, USA) was used for the above statistical analyses.

Results

Variations of DSC and OI

During the 6-week long treatment course, the DSC decreased as an increasing number of fractions were delivered (*Table 1*). The DSC of the $GTV_{\_Ns}$, $GTV_{\_Nl}$, and GTV_T were <70% after the first, second, and third week, respectively. For all the TVs, the changes of OI had a similar time-trend with those of DSC (*Table 1*). For all TVs of primary tumors and lymph nodes, the DSC differences between the various weeks were statistically significant (P<0.05) (*Table 1*). Comparing the OI and DSC in the concurrent and sequential CRT subgroups, the OI, and DSC values were smaller in the concurrent subgroup. Moreover, the majority of OIs and DSCs showed a significant statistical difference between concurrent and sequential treatment (*Table 2*).

Variations of the mean of SPDs and overall SD

For the quantitation of contour surface features, the mean SPD showed an increasing time trend, i.e., the SPD between two TVs on the pCT and rCT images increased with increasing numbers of radiation fractions delivered over the course of the treatment. For the GTV of the primary tumor and neck lymph nodes, all the mean SPDs were 1.5–2.5 mm during the first week and 5.2–6.2 mm during the last week (*Figure 2A*). Similarly, overall SD, as a measure of overall differences, increased significantly from the first week to the last week (*Figure 2B*). The SPDs and overall SDs were larger in the CRT subgroup than in the sequential therapy subgroup (*Table 2*).

Expanded margins

When the expanded margin increased from 1 to 5 mm, the absolute volume of the PTV increased from 15.1% to 104.8%. The volume of PTV had a 13.0–18.8% increase with the addition of each millimeter expansion (*Figure 3*). If there was no margin expansion, not all of the OIs were higher than 0.95. More than 95% of the OIs were >0.95 in the first three weeks when the margin was expanded by 1 mm. When the margin was expanded by 2 mm, all OIs were higher than 0.95 throughout the six-week-long treatment course (*Figure 4*).

Discussion

Currently, a large selection of parameters based on different formalisms has been used for the evaluation of contour variability (22,24,25). Volumetric parameters, such as OI, Jaccard conformity index, and DSC (22), and positional parameters (4,5), such as system or random set-up errors and displacement of center of mass, have been used to describe contour geometrical variations (4). Recently, 3-dimensional shape representation parameters, such as the distance to corresponding surface points, have been employed as shape metrics (24). Due to different calculations, the conformity index usually provides a low value (high variability), while the DSC can provide a false impression of high agreement when used as a concordance measure (25). In this study, we used the volumetric (OI and DSC) and surface distance parameters (the SPD) to quantify the tumor variability during the course of CRT.

Deformable image registration is a useful technique to account for complex internal anatomical variation and to estimate the shape variability for a contour. It can track each corresponding voxel of all anatomical structures for contour propagation and dose accumulation during radiation treatment (12). Twelve patients with head and neck cancer who were treated with dose painting IMRT had been used to evaluate the accuracy of deformable registrations (20). All TVs were contoured manually on both the pCT and rCT images. After the deformable registration, contour comparison was performed between TVs propagated automatically and those delineated manually. After a median dose of 30 Gy was delivered, the Jaccard conformity index of the GTV and CTV were 0.4–0.8 and 0.8–0.9, respectively and those of OIs were 0.6–0.7 and 0.8, respectively. In a study by Zhang *et al.* (30), deformable

Table 1 The shape presentation parameters of all TVs in different week (mean ± SD, 95% CI)

Parameters	TV	Week						Mean
		1st	2nd	3rd	4th	5th	6th	
$OI_{\_pCT}$	$GTV_{\_T}$	0.81±0.09 (0.77, 0.86)	0.71±0.12 (0.65, 0.76)	0.61±0.15 (0.55, 0.68)	0.55±0.16 (0.48, 0.63)	0.48±0.15 (0.41, 0.56)	0.43±0.15 (0.36, 0.51)	0.60±0.19 (0.57, 0.64)*
	$GTV_{\_Nl}$	0.71±0.23 (0.51, 0.90)	0.59±0.24 (0.39, 0.79)	0.47±0.26 (0.25, 0.68)	0.41±0.24 (0.21, 0.68)	0.35±0.23 (0.16, 0.54)	0.32±0.21 (0.14, 0.49)	0.47±0.26 (0.40, 0.55)*
	$GTV_{\_Ns}$	0.62±0.18 (0.54, 0.69)	0.49±0.16 (0.43, 0.56)	0.38±0.17 (0.31, 0.45)	0.31±0.16 (0.25, 0.38)	0.29±0.15 (0.23, 0.35)	0.25±0.16 (0.18, 0.32)	0.39±0.20 (0.36, 0.42)*
	$CTV_{\_Lr}$	0.93±0.04 (0.91, 0.95)	0.92±0.04 (0.91, 0.94)	0.90±0.04 (0.88, 0.92)	0.89±0.05 (0.87, 0.91)	0.87±0.04 (0.85, 0.89)	0.86±0.04 (0.84, 0.88)	0.90±0.05 (0.89, 0.91)*
$OI_{\_rCT}$	$GTV_{\_T}$	0.98±0.02 (0.97, 0.99)	0.97±0.02 (0.96, 0.98)	0.97±0.03 (0.95, 0.98)	0.96±0.03 (0.95, 0.98)	0.96±0.03 (0.95, 0.98)	0.96±0.04 (0.94, 0.98)	0.97±0.03 (0.96, 0.97)
	$GTV_{\_Nl}$	0.96±0.03 (0.94, 0.98)	0.95±0.03 (0.92, 0.98)	0.93±0.06 (0.88, 0.99)	0.93±0.07 (0.87, 0.99)	0.93±0.08 (0.86, 1.00)	0.92±0.08 (0.99, 0.85)	0.94±0.06 (0.92, 0.96)
	$GTV_{\_Ns}$	0.86±0.11 (0.82, 0.91)	0.84±0.12 (0.79, 0.89)	0.80±0.21 (0.71, 0.88)	0.78±0.22 (0.69, 0.88)	0.77±0.20 (0.69, 0.85)	0.74±0.27 (0.62, 0.85)	0.80±0.20 (0.77, 0.86)
	$CTV_{\_Lr}$	0.95±0.03 (0.94, 0.96)	0.95±0.02 (0.94, 0.96)	0.95±0.02 (0.93, 0.95)	0.94±0.02 (0.93, 0.95)	0.94±0.03 (0.92, 0.95)	0.93±0.03 (0.92, 0.95)	0.94±0.03 (0.94, 0.95)*
DSC†	$GTV_{\_T}$	0.89±0.06 (0.86, 0.91)	0.81±0.09 (0.77, 0.85)	0.74±0.11 (0.69, 0.79)	0.69±0.13 (0.63, 0.75)	0.63±0.14 (0.56, 0.70)	0.58±0.14 (0.52, 0.65)	0.72±0.15 (0.70, 0.75)*
	$GTV_{\_Nl}$	0.79±0.17 (0.65, 0.93)	0.70±0.20 (0.54, 0.87)	0.59±0.24 (0.39, 0.79)	0.54±0.23 (0.35, 0.73)	0.48±0.23 (0.29, 0.67)	0.44±0.22 (0.26, 0.63)	0.59±0.24 (0.52, 0.66)*
	$GTV_{\_Ns}$	0.70±0.15 (0.64, 0.77)	0.61±0.14 (0.55, 0.66)	0.50±0.18 (0.42. 0.57)	0.43±0.18 (0.36, 0.50)	0.41±0.18 (0.33, 0.48)	0.36±0.20 (0.27, 0.54)	0.50±0.21 (0.44, 0.54)*
	$CTV_{\_Lr}$	0.94±0.03 (0.93, 0.96)	0.94±0.02 (0.93, 0.95)	0.92±0.03 (0.91, 0.94)	0.91±0.03 (0.90, 0.93)	0.90±0.03 (0.89, 0.92)	0.89±0.03 (0.88, 0.91)	0.92±0.03 (0.91, 0.92)*
Mean SPD† (mm)	$GTV_{\_T}$	1.5±0.8 (1.1, 1.8)	2.4±1.2 (1.9, 3.0)	3.3±1.6 (2.6, 4.0)	4.2±2.1 (3.2, 5.2)	5.0±2.3 (4.0, 6.1)	5.8±2.5 (4.6, 7.0)	3.7±2.3 (3.3, 4.1)*
	$GTV_{\_Nl}$	2.3±2.0 (0.6, 4.0)	3.4±2.2 (1.5, 5.2)	4.8±2.6 (2.6, 6.9)	5.3±2.5 (3.7, 7.4)	5.9±2.4 (3.8, 7.9)	6.3±2.4 (4.3, 8.3)	4.6±2.6 (3.9, 5.4)*
	$GTV_{\_Ns}$	1.9±1.1 (1.5, 2.4)	2.6±1.0 (2.2, 3.1)	3.4±1.2 (2.9, 3.8)	3.9±1.3 (3.4, 4.4)	4.2±1.6 (3.5, 4.9)	5.2±3.5 (3.7, 6.7)	3.5±2.1 (3.2, 3.9)*
	$CTV_{\_Lr}$	1.0±0.5 (0.8, 1.3)	1.1±0.5 (0.9, 1.3)	1.4±0.5 (1.1, 1.6)	1.6±0.6 (1.3, 1.9)	1.7±0.6 (1.4, 2.0)	1.9±0.6 (1.6, 2.2)	1.4±0.6 (1.3, 1.6)*
Overall SD† (mm)	$GTV_{\_T}$	2.2±1.2 (1.7, 2.8)	3.0±1.2 (2.4, 3.6)	3.5±1.5 (2.8, 4.2)	4.1±1.9 (3.2, 5.0)	4.7±1.9 (3.8, 5.6)	5.2±2.4 (4.1, 6.3)	3.7±2.3 (3.3, 4.1)*
	$GTV_{\_Nl}$	2.1±1.2 (1.1, 3.1)	2.7±1.1 (1.8, 3.6)	3.6±1.3 (2.5, 4.8)	3.7±1.2 (2.7, 4.7)	3.9±1.2 (2.8, 4.9)	3.9±1.2 (2.9, 4.9)	3.3±1.3 (2.9, 3.7)*
	$GTV_{\_Ns}$	1.8±0.8 (1.9, 2.6)	2.2±0.7 (1.9, 2.6)	2.6±0.9 (2.3, 3.0)	2.9±0.9 (2.6, 3.3)	3.2±1.3 (2.6, 3.7)	4.0±3.2 (2.7, 5.4)	2.8±1.7 (2.5, 3.1)*
	$CTV_{\_Lr}$	2.1±0.8 (1.7, 2.5)	2.1±0.7 (1.8, 2.4)	2.4±0.7 (2.1, 2.7)	2.6±0.8 (2.2, 3.0)	2.8±0.8 (2.4, 3.1)	3.0±0.9 (2.6, 3.4)	2.5±0.8 (2.4, 2.7)*

OI of the initial volume on pCT calculated by $TV_{\_common}/TV_{\_pCT}$ ($OI_{\_pCT}$) or $TV_{\_common}/TV_{\_rCT}$ ($OI_{\_rCT}$); $TV_{\_pCT}$, $TV_{\_rCT}$, and $TV_{\_common}$ are the initial volume on the planning CT, the volume delineated manually on repeat CTs, and their common volumes, respectively. †, the OI and DSC was calculated as $2\times TV_{\_common}/(TV_{\_rCT}+TV_{\_pCT})$. And mean SPD is the mean surface distances between TVs in rCT and its pCT. Overall SD was calculated as the SD of all the SPDs from each point in the surface of TV delineated in rCT image; *, P value <0.05 when comparing among different weeks with one-way analysis of variance. TV, target volume; SD, standard deviation; 95% CI, 95% confidence interval; $GTV_{\_T}$, GTV of the primary tumor; $GTV_{\_Nl}$, GTV of a large lymph node; $CTV_{\_Nl}$, CTV of a large lymph node (the shortest diameter >3.0 cm); $GTV_{\_Ns}$, GTV of a small lymph node (>1 cm and ≤3 cm); $CTV_{\_Lr}$, CTV of a low risk region; CRT, chemoradiotherapy; SPD, the shortest perpendicular distance; OI, overlapping index; DSC, dice similarity coefficient; GTV, gross tumor volume; CTV, clinical target volume.

Table 2 The shape presentation parameters of all TVs in concurrent and sequential chemoradiotherapy subgroup (mean ± SD, 95% CI)

Parameters	GTV_{T}			GTV_{Nl}			GTV_{Ns}			CTV_{Lr}		
	Seq	Con	P value	Seq	Con	P value	Seq	Con	P value	Seq	Con	P value
OI_{pCT}	0.62±0.18 (0.58, 0.67)	0.56±0.19 (0.50, 0.62)	0.074	0.75±0.18 (0.64, 0.86)	0.38±0.22 (0.31, 0.46)	0.000	0.53±0.15 (0.47, 0.59)	0.36±0.20 (0.33, 0.40)	0.000	0.92±0.04 (0.91, 0.93)	0.89±0.05 (0.887, 0.90)	0.000
OI_{rCT}	0.98±0.02 (0.97, 0.98)	0.96±0.04 (0.95, 0.97)	0.019	0.98±0.01 (0.98, 0.98)	0.92±0.07 (0.90, 0.95)	0.004	0.89±0.07 (0.86, 0.92)	0.78±0.21 (0.74, 0.82)	0.010	0.95±0.03 (0.94, 0.95)	0.94±0.03 (0.94, 0.95)	0.360
DSC	0.74±0.15 (0.71, 0.77)	0.69±0.16 (0.64,0.74)	0.091	0.84±0.13 (0.76, 0.92)	0.51±0.21 (0.44, 0.58)	0.000	0.66±0.13 (0.61, 0.72)	0.47±0.21 (0.44, 0.51)	0.000	0.93±0.03 (0.92, 0.94)	0.91±0.03 (0.80, 0.92)	0.002
Mean SPD (mm)	3.4±2.1 (3.0, 3.9)	4.2±2.7 (3.4, 5.1)	0.074	2.6±1.6 (1.5, 3.6)	5.3±2.6 (4.5, 6.2)	0.001	2.5±0.7 (2.2, 2.8)	3.7±2.2 (3.3, 4.1)	0.007	1.2±0.5 (1.0, 1.3)	1.6±0.6 (1.4, 1.7)	0.001
Overall SD (mm)	3.5±1.7 (3.1, 3.9)	4.3±2.4 (3.6, 5.1)	0.027	2.8±1.3 (2.0, 3.7)	3.5±1.3 (3.0, 3.9)	0.157	2.3±0.5 (2.1, 2.5)	2.8±1.6 (2.5, 3.1)	0.086	2.1±0.7 (1.9, 2.3)	2.7±0.8 (2.5, 2.9)	0.000

TV, target volume; SD, standard deviation; 95% CI, 95% confidence interval; Seq, sequential chemoradiotherapy; Con, concurrent chemoradiotherapy; GTV_{T}, GTV of the primary tumor; GTV_{Nl}, GTV of a large lymph node; GTV_{Ns}, GTV of a small lymph node (>1 and ≤3 cm); CTV_{Lr}, CTV of a low risk region; CRT, chemoradiotherapy; SPD, the shortest perpendicular distance; OI, overlapping index; DSC, dice similarity coefficient; GTV, gross tumor volume; CTV, clinical target volume.

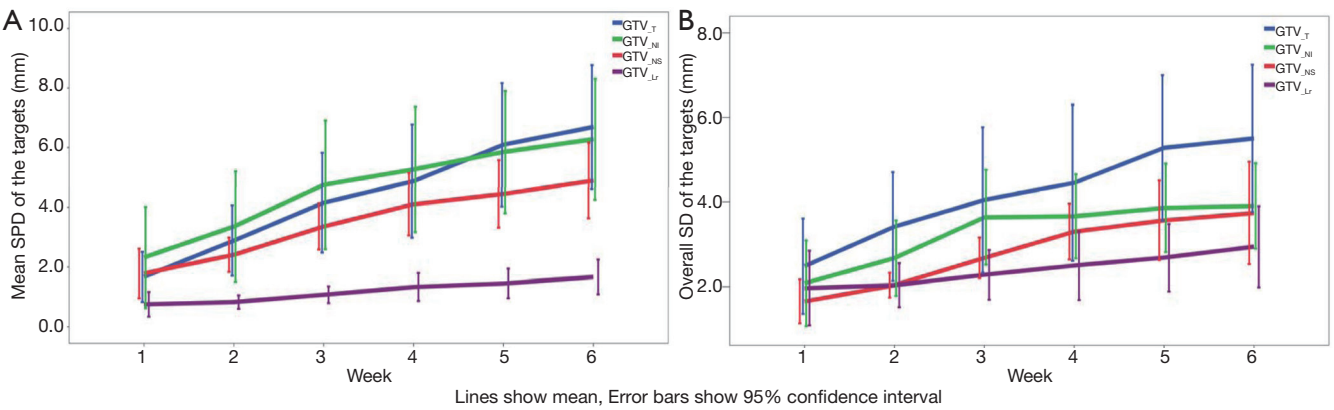

Figure 2 The mean SPD (A) and overall SD (B) in different weeks. SPD, shortest perpendicular distance; SD, standard deviation; GTV_{T}, gross tumor volume of the primary tumor; GTV_{Nl}, GTV of a large lymph node; GTV_{Ns}, GTV of a small lymph node; CTV_{Lr}, low-risk CTV region; GTV, gross tumor volume.

registrations of cone-beam CT images of 20 patients with head and neck cancer were implemented while 40 or 50 Gy was delivered. The median DSC was 0.55 for the lymph nodal GTV. In our study, the OI had the same definition as the OI in Olteanu's study (20), and the OI in our study had a similar trend to decrease over time. For the GTV of the primary tumor and neck lymph nodes, the OI in the fourth or fifth week were approximately 0.30–0.55 in this study.

All of the DSCs, OI, and SPDs, in addition to overall SDs, showed a consecutive variation time trend throughout the course of treatment. Generally, a DSC value >0.7 represents excellent agreement (25). The DSCs of all GTVs in this study were lower than 0.7, indicating the shape of the tumor underwent considerable changes and a reasonable re-planning was thus necessary. In our study, the GTVs of the primary tumor and lymph nodes were less than 0.7 after the first three weeks. In our previous study (4), the volume loss of the primary tumor and lymph nodes was also more than 50% in the first half of treatment course, which suggests that the volumetric coverage variations occurred earlier than volumetric loss. One of the possible explanations was that volumetric loss, positional shift and contour misalignment

might have contributed to the overlapping parameters variations. Furthermore, all DSC values of all TVs in the concurrent CRT subgroup showed lower values, which suggests that the adaptive strategy should differ according to the treatment modality.

A surface-based analysis allows for visualization of contour disagreement (25). Recently, Hamming-Vrieze *et al*. (23) used implanted gold markers to evaluate shape variations in tumors of 27 patients with oropharyngeal tumors during RT. After a bony registration between cone-beam and treatment pCT, the markers were positioned at the edge of the GTV at a depth of 5 mm, and a 3-dimensional vector of the markers' daily motions was used to determine the amplitude of the surface deformations. The 3-dimensional vector of the marker displacement was 2.3 mm on average and depended on the sub-location and volume of the tumor. Using contour comparisons with various statistical shape models, one can be used to represent contour shape variability between images (24). The surface distance in our study was developed from corresponding points on the TV surface in each rCT and pCT. The mean SPD of GTVs ranged from 1.5 to 4.6 mm and that of CTV_{Lr} was 1–2 mm, with an increasing trend over time. Regarding the change of overall SD, the TV in rCT had an increasing difference with that in pCT.

However, the tumor shrinkage observed for head and neck cancer does not result in significant dosimetric differences in TVs (18). The combination of re-planning and reduced margins might probably provide mote benefits both to the tumor and healthy tissue.

In this study, we used geometrical coverage as surrogate to estimate the margin by weekly repeat CT imaging rigid

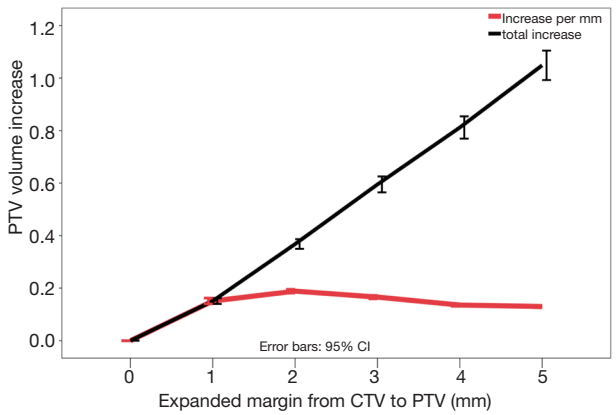

Figure 3 The volume increase and the expanded margin. The total increase of PTV was calculated by $(V_{\_PTV\_x} - V_{\_PTV\_0})/ V_{\_PTV\_0} \times 100\%$, and the volume increase per millimeter was calculated by $(V_{\_PTV\_x} - V_{\_PTV\_x\text{-}1})/V_{\_PTV\_x\text{-}1}$ (x=1, 2, 3, 4, 5). PTV, planning target volume; $V_{\_PTV\_0}$, the volume of $CTV_{\_Lr}$ in pCT; CTV, clinical target volume; pCT, planning CT; $CTV_{\_Lr}$, low-risk CTV region.

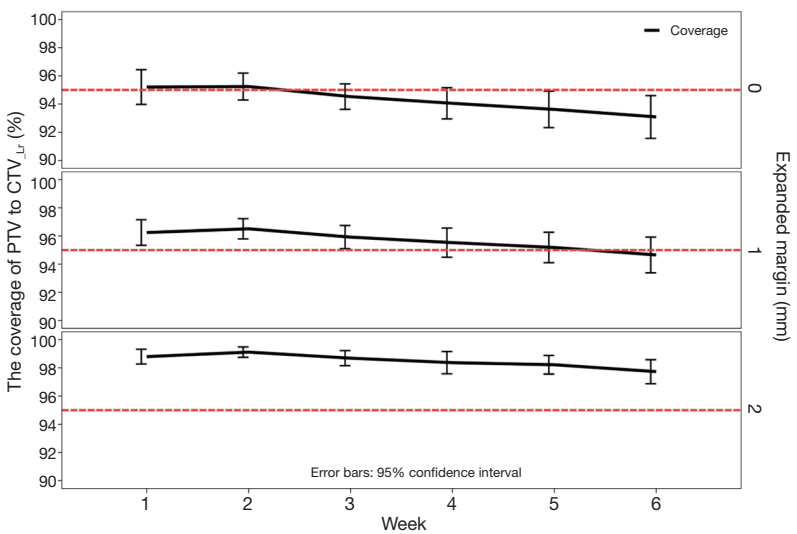

Figure 4 The expanded margin to maintain the desired geometrical coverage. The overlapping percentage of PTV that expanded from $CTV_{\_Lr}$ in pCT with 0, 1, and 2 mm and the $CTV_{\_Lr}$ volume in rCT. For the overlapping percentage, the lower limits of 95% confidence interval higher than 95% were defined as acceptable geometrical coverage. PTV, planning target volume; $CTV_{\_Lr}$, low-risk clinical target volume; pCT, planning CT; rCT, repeat CT.

registration while without taking the set-up performance and TV delineation variability into account. If there is no additional margin, the geometrical coverage seems to be inadequate. A 2-mm margin expansion could maintain geometrical coverage of >95% during the whole treatment course, and a 1 mm margin expansion could maintain that coverage no later than the third week of the treatment course. Regardless of a few factors, such as tumor shrinkage and deformations in head and neck anatomy, re-mapping of the contours via imaging registration might contribute to the accuracy of the volume overlap; in this study, we tried to reproduce the procedures of weekly CT-guided IMRT for NPC in our daily practice and to analyze the geometrical changes that occurred during the treatment course. The margin reduction we recommended in this study might be useful for the adaptive re-planning of NPC treatment. Though a dosimetric evaluation might be necessary for the final decision-making of the adaptive treatment, it should be based on the appropriate definition of all the targets and organs at risk.

A few limitations remain in our study. The accuracy verification of the contour alignments between pCT and rCT, imaging quality without contrast in rCT, intra-observer delineation variability in different images, and microscopic disease movement during the treatment were not addressed. The dosimetric variations from geometrical changes are usually the main end-result and decisive factors in decision-making, and these were not included in this study. Theoretically, the geometrical variation during radiation treatment is also important for adaptive radiotherapy, which could be used to guide the re-delineation of the targets and the selection of re-planning timing. Despite these drawbacks, to the best of our knowledge, this is the first study to quantify the consecutive tumor geometric coverage and surface variations during chemoradiation therapy and to investigate the strategy of margin reduction that might be useful to the adaptive therapy of head and neck cancer.

Conclusions

Considerable tumor geometric coverage and surface variations occurred during CRT for patients with locally advanced NPC. The overlapping parameters decreased and the surface distance increased as the number of fractions delivered increased throughout the treatment course. The DSCs of GTVs were <0.7 in the first half of the treatment course. These time trends of tumor variations suggested that appropriate adaption to the anatomical changes might be necessary early in the therapy course. Margins should be expanded by 2 mm to maintain acceptable geometrical coverage throughout the CRT course and by 1 mm margin to maintain coverage if geometrical adaption such as re-planning was undertaken in the first three weeks of the treatment course, without taking the delineation and registration uncertainties and set-up performance into account. Therefore, re-planning before the third week, i.e., no more than approximately 30 Gy delivered, might result in margin reduction and spare more healthy tissues from receiving an unnecessary high radiation dose. Future research topics should include how these geometrical variations and the adaptive strategies may be translated into the dosimetric and clinical benefits to the tumors and/or organs at risk.

Acknowledgements

We are grateful to Jan-Jakob Sonke from the Department of Radiation Oncology, The Netherlands Cancer Institute, Amsterdam, The Netherlands, who generously offered the research software developed in-house for this research.
Funding: This study was funded by Wuhan Science & technique grant 2015060101010054 and Hubei Healthy funding WJ2015Q027.

Footnote

Conflicts of Interest: This study was presented as digital poster at the 2014 Annual Meeting of the European Society of Radiotherapy & Oncology, Vienna, Austria, April 4–8, 2014.

Ethical Approval: All procedures performed in studies involving human participants were in accordance with the ethical standards of the institutional and/or national research committee and with the 1964 Helsinki declaration and its later amendments or comparable ethical standards. And Informed consent was obtained from all individual participants included in the study.

References

1. Lee AW, Ng WT, Chan YH, Sze H, Chan C, Lam TH. The battle against nasopharyngeal cancer. Radiother Oncol 2012;104:272-8.
2. Lee AW, Lin JC, Ng WT. Current management of

nasopharyngeal cancer. Semin Radiat Oncol 2012;22:233-44.
3. Castadot P, Lee JA, Geets X, Grégoire V. Adaptive radiotherapy of head and neck cancer. Semin Radiat Oncol 2010;20:84-93.
4. Tan W, Li Y, Han G, Xu J, Wang X, Li Y, Hu D. Target volume and position variations during intensity-modulated radiotherapy for patients with nasopharyngeal carcinoma. Onco Targets Ther 2013;6:1719-28.
5. Barker JL Jr, Garden AS, Ang KK, O'Daniel JC, Wang H, Court LE, Morrison WH, Rosenthal DI, Chao KS, Tucker SL, Mohan R, Dong L. Quantification of volumetric and geometric changes occurring during fractionated radiotherapy for head-and-neck cancer using an integrated CT/linear accelerator system. Int J Radiat Oncol Biol Phys 2004;59:960-70.
6. Wang X, Lu J, Xiong X, Zhu G, Ying H, He S, Hu W, Hu C. Anatomic and dosimetric changes during the treatment course of intensity-modulated radiotherapy for locally advanced nasopharyngeal carcinoma. Med Dosim 2010;35:151-7.
7. Zhang X, Li M, Cao J, Luo JW, Xu GZ, Gao L, Yi J, Huang X, Xiao J, Li S, Dai J. Dosimetric variations of target volumes and organs at risk in nasopharyngeal carcinoma intensity-modulated radiotherapy. Br J Radiol 2012;85:e506-13.
8. Yang H, Hu W, Ding W, Shan G, Wang W, Yu C, Wang B, Shao M, Wang J, Yang W. Changes of the transverse diameter and volume and dosimetry before the 25th fraction during the course of intensity-modulated radiation therapy (IMRT) for patients with nasopharyngeal carcinoma. Med Dosim 2012;37:225-9.
9. Wang RH, Zhang SX, Zhou LH, Zhang GQ, Yu H, Lin XD, Lin S. Volume and dosimetric variations during two-phase adaptive intensity-modulated radiotherapy for locally advanced nasopharyngeal carcinoma. Biomed Mater Eng 2014;24:1217-25.
10. Lu J, Ma Y, Chen J, Wang L, Zhang G, Zhao M, Yin Y. Assessment of anatomical and dosimetric changes by a deformable registration method during the course of intensity-modulated radiotherapy for nasopharyngeal carcinoma. J Radiat Res 2014;55:97-104.
11. Cheng HC, Wu VW, Ngan RK, Tang KW, Chan CC, Wong KH, Au SK, Kwong DL. A prospective study on volumetric and dosimetric changes during intensity-modulated radiotherapy for nasopharyngeal carcinoma patients. Radiother Oncol 2012;104:317-23.
12. Castadot P, Geets X, Lee JA, Christian N, Grégoire V. Assessment by a deformable registration method of the volumetric and positional changes of target volumes and organs at risk in pharyngo-laryngeal tumors treated with concomitant chemo-radiation. Radiother Oncol 2010;95:209-17.
13. Zhao L, Wan Q, Zhou Y, Deng X, Xie C, Wu S. The role of replanning in fractionated intensity modulated radiotherapy for nasopharyngeal carcinoma. Radiother Oncol 2011;98:23-7.
14. Wang W, Yang H, Hu W, Shan G, Ding W, Yu C, Wang B, Wang X, Xu Q. Clinical study of the necessity of replanning before the 25th fraction during the course of intensity-modulated radiotherapy for patients with nasopharyngeal carcinoma. Int J Radiat Oncol Biol Phys 2010;77:617-21.
15. Yang H, Tu Y, Wang W, Hu W, Ding W, Yu C, Zhou C. A comparison of anatomical and dosimetric variations in the first 15 fractions, and between fractions 16 and 25, of intensity-modulated radiotherapy for nasopharyngeal carcinoma. J Appl Clin Med Phys 2013;14:3918.
16. Schwartz DL, Garden AS, Thomas J, Chen Y, Zhang Y, Lewin J, Chambers MS, Dong L. Adaptive radiotherapy for head-and-neck cancer: initial clinical outcomes from a prospective trial. Int J Radiat Oncol Biol Phys 2012;83:986-93.
17. Schwartz DL. Current progress in adaptive radiation therapy for head and neck cancer. Curr Oncol Rep 2012;14:139-47.
18. Wu Q, Chi Y, Chen PY, Krauss DJ, Yan D, Martinez A. Adaptive replanning strategies accounting for shrinkage in head and neck IMRT. Int J Radiat Oncol Biol Phys 2009;75:924-32.
19. Yang H, Hu W, Wang W, Chen P, Ding W, Luo W. Replanning during intensity modulated radiation therapy improved quality of life in patients with nasopharyngeal carcinoma. Int J Radiat Oncol Biol Phys 2013;85:e47-54.
20. Olteanu LA, Madani I, De Neve W, Vercauteren T, De Gersem W. Evaluation of deformable image coregistration in adaptive dose painting by numbers for head-and-neck cancer. Int J Radiat Oncol Biol Phys 2012;83:696-703.
21. Piotrowski T, Ryczkowski A, Kazmierska J. B-Spline registration based on new concept of an intelligent masking procedure and GPU computations for the head and neck adaptive tomotherapy. Technol Cancer Res Treat 2012;11:257-66.
22. Castadot P, Lee JA, Parraga A, Geets X, Macq B, Grégoire V. Comparison of 12 deformable registration strategies in adaptive radiation therapy for the treatment of head and neck tumors. Radiother Oncol 2008;89:1-12.

23. Hamming-Vrieze O, van Kranen SR, van Beek S, Heemsbergen W, van Herk M, van den Brekel MW, Sonke JJ, Rasch CR. Evaluation of tumor shape variability in head-and-neck cancer patients over the course of radiation therapy using implanted gold markers. Int J Radiat Oncol Biol Phys 2012;84:e201-7.
24. Heimann T, Meinzer HP. Statistical shape models for 3D medical image segmentation: a review. Med Image Anal 2009;13:543-63.
25. Fotina I, Lütgendorf-Caucig C, Stock M, Pötter R, Georg D. Critical discussion of evaluation parameters for inter-observer variability in target definition for radiation therapy. Strahlenther Onkol 2012;188:160-7.
26. Zhang H, Tan W, Sonke JJ. Effect of compressed sensing reconstruction on target and organ delineation in cone-beam CT of head-and-neck and breast cancer patients. Radiother Oncol 2014;112:413-7.
27. Balik S, Weiss E, Jan N, Roman N, Sleeman WC, Fatyga M, Christensen GE, Zhang C, Murphy MJ, Lu J, Keall P, Williamson JF, Hugo GD. Evaluation of 4-dimensional computed tomography to 4-dimensional cone-beam computed tomography deformable image registration for lung cancer adaptive radiation therapy. Int J Radiat Oncol Biol Phys 2013;86:372-9.
28. Steenbakkers RJ, Duppen JC, Fitton I, Deurloo KE, Zijp L, Uitterhoeve AL, Rodrigus PT, Kramer GW, Bussink J, De Jaeger K, Belderbos JS, Hart AA, Nowak PJ, van Herk M, Rasch CR. Observer variation in target volume delineation of lung cancer related to radiation oncologist-computer interaction: a 'Big Brother' evaluation. Radiother Oncol 2005;77:182-90.
29. van Herk M. Errors and margins in radiotherapy. Semin Radiat Oncol 2004;14:52-64.
30. Zhang T, Chi Y, Meldolesi E, Yan D. Automatic delineation of on-line head-and-neck computed tomography images: toward on-line adaptive radiotherapy. Int J Radiat Oncol Biol Phys 2007;68:522-30.

Cite this article as: Tan W, Ye J, Xu R, Li X, He W, Wang X, Li Y, Hu D. The tumor shape changes of nasopharyngeal cancer during chemoradiotherapy: the estimated margin to cover the geometrical variation. Quant Imaging Med Surg 2016;6(2):115-124. doi:10.21037/qims.2016.03.07

